J Mater Sci: Mater Electron (2008) 19:669–675
DOI 10.1007/s10854-007-9419-x

Influence of Mn on dielectric and piezoelectric properties of A-site and B-site modified PLZT nano-ceramics for sensor and actuator applications

Ramam Koduri · Marta Lopez

Received: 13 June 2007 / Accepted: 24 September 2007 / Published online: 16 October 2007

Abstract $[Pb_{0.961}La_{0.012}Ba_{0.015}Sr_{0.012}][Zr_{0.53}Ti_{0.47}]_{0.967-(h/2)}Nb_{0.02}Zn_{0.01}Mn_hO_3$ (PLBSZZMNT) nano-ceramics where h = 0, 0.5. 1 and 1.5 mol% fabricated through solid state reaction method has been investigated for phase formation, microstructure, density, dielectric and piezoelectric properties. X-ray diffraction studies indicated that all the samples exhibited a single-phase perovskite tetragonal structure which had strongly intensified due to the acceptor Mn content increment in the series. Our investigation with reference to isovalent (Ba^{2+} and Sr^{2+}) on the A-site, pentavalent donor (Nb^{5+}) and acceptor (Zn^{2+} and Mn^{4+}) dopants on the B-site in PLZT perovskite with the stoichiometric compositional formulation tailored for dielectric and piezoelectric properties has been clearly explained. As Mn concentration increased, the grain growth enhanced, and the inter-diffusion between multiple ions promoted densification in the PLBSZZMNT nano-ceramics. TEM studies revealed an average particle size ranging from 20 to 72 nm. Dielectric characterization revealed that the ε_{RT} enhanced till 1.5 mol% Mn (2946) while the Curie temperature and dielectric loss at room temperature (T_c and $Tan\delta_{RT}$) decreased, respectively. Mn doping in PLBSZZNT induced the piezoelectric parameters (k_p = 0.567) and (d_{33} = 486 pC/N) till 1.5 mol% Mn. Thus, 1.5 mol% Mn modified PLBSZZNT exhibits optimum dielectric and piezoelectric properties, which are suitable for possible sensor and actuator applications.

R. Koduri (✉) · M. Lopez
Departmento de Ingeneria de Materials (DIMAT), Facultad de Ingenieria, Universidad de Concepcion, Concepcion, Chile
e-mail: ramamk@udec.cl

1 Introduction

Lead Zirconate Titanate (PZT) is a binary solid solution of $PbZrO_3$ and $PbTiO_3$ having a perovskite type structure with Pb^{2+} ions occupying the A-site, and the Zr^{4+} and Ti^{4+} ions occupying the B site. PZT in combination with different dopants exhibited outstanding electromechanical properties in either bulk or thin films depending on the customized properties for an extensive range of applications [1–3]. These ferroelectric ceramics have been used in diverse areas such as, dielectric ceramics for capacitor applications, ferroelectric ceramics or thin films for non-volatile memory applications, piezoelectric ceramics for sensors and actuators or electro-optic materials for data storage and displays.

PZT in conjunction with various types of dopants have been synthesized through different methods for specific properties desired. PZT has been studied with varied dopants like Zn, Sr and Y [4], Ba [5], Nb [6], Mn [7], La [8], PMS-PZT [9], PMN-PZT [10], PZN-PZT [11], ZnO [12], PZN-PT [13], PNW-PMN-PZT [14], PZNT [15], PZN [16], Nd [17], Zn [18] etc. The hard doping ions like Mn^{2+}/Mn^{3+} which occupy the B-site in the perovskite structure had been investigated [19, 20]. Manganese-doped PZT thin films prepared through sol-gel technique was studied by Zhang et al. [21].

The physical mechanism of hard doping is complex, since different hard doping ions affect different properties especially a ternary ceramic system with Mn doping has an enhanced quality mechanical factor (Q_m) and an almost unchanged (k_p) piezoelectric planar coupling coefficient. A hard doping ion is considered an acceptor, since it causes oxygen vacancies in the perovskite lattice. The hard doping ion may be occupied either in A or B-site, depending upon the ionic radius of the doping ion, which usually has a

Table 1 Stoichiometric compositions synthesized

Composition	Formulae
General formula	$[Pb_{1-w-x-y}La_wBa_xSr_y][Zr_zTi_{1-z}]_{1-(w/4)-(5k/4)-(m/2)-(h/2)}Nb_kZn_mMn_hO_3$
mol%	w = La = 1.2, x = Ba = 1.5, y = Sr = 1.2, z = Zr = 53, 1–z = Ti = 47, k = Nb = 2, m = Zn = 1 and h = Mn = 0, 0.5, 1 and 1.5
PLBSZZMNT	$[Pb_{0.961}La_{0.012}Ba_{0.015}Sr_{0.012}][Zr_{0.53}Ti_{0.47}]_{0.967-(h/2)}Nb_{0.02}Zn_{0.01}Mn_hO_3$
h = 0	$[Pb_{0.961}La_{0.012}Ba_{0.015}Sr_{0.012}][Zr_{0.53}Ti_{0.47}]_{0.967}Nb_{0.02}Zn_{0.01}O_3$
h = 0.5	$[Pb_{0.961}La_{0.012}Ba_{0.015}Sr_{0.012}][Zr_{0.53}Ti_{0.47}]_{0.9645}Nb_{0.02}Zn_{0.01}Mn_{0.005}O_3$
h = 1.0	$[Pb_{0.961}La_{0.012}Ba_{0.015}Sr_{0.012}][Zr_{0.53}Ti_{0.47}]_{0.962}Nb_{0.02}Zn_{0.01}Mn_{0.01}O_3$
h = 1.5	$[Pb_{0.961}La_{0.012}Ba_{0.015}Sr_{0.012}][Zr_{0.53}Ti_{0.47}]_{0.9595}Nb_{0.02}Zn_{0.01}Mn_{0.015}O_3$

lower or equal chemical valence or approximately similar ionic radii than that of the ion replaced in the lattice [2]. Using element substitution, one can tailor the properties of the ceramics for any specific application desired.

This paper highlights influence of donors and acceptors modified PLZT nano-ceramics for the phase evolution, microstructure, density profile, dielectric and piezoelectric properties. Introduction of isovalent (Ba^{2+} and Sr^{2+}) cations at the A-site and donor pentavalent (Nb^{5+}), acceptor (Zn^{2+} and Mn^{4+}) cations at the B-site in the piezoelectric lead lanthanum zirconium titanate solid solutions were characterized. The combined effects of all these donor and acceptor dopants were analyzed and characterized. The general chemical formulae and compositions synthesized have been presented in Table 1.

2 Experimental procedure

2.1 Ceramic processing

Analytical reagent grade powders (purity 99.99%) of PbO, La_2O_3, $BaCO_3$, $SrCO_3$, ZrO_2, ZnO, Nb_2O_5, TiO_2 and MnO_2 were used as starting materials and the solid solutions were prepared through solid state reaction method. The weighed starting reagents were mixed in appropriate stoichiometric ratios. Initially, all the batch compositions were added with excess 2–6 wt% PbO and were synthesized. These nano-ceramic compositions (final materials) were characterized for phase formation, microstructure features and density. These compositions with excess 4 wt% and 6 wt% PbO were not consistent in phase formation, whereas, 5 wt% PbO added compositions had shown consistency in phase formation since starting stoichiometric materials participate in the chemical reaction to form end product, while excess PbO compensates the lead volatilization during high temperature sintering. Thus, 5 wt% excess PbO was added in all PLBSZZMNT compositions.

The batch powders were ball milled using zirconia balls and ethanol as media for 24 h. The dried powders were calcined at 935 °C for 3 h in a high purity alumina crucible by maintaining air atmosphere. Calcined powders were ball milled using zirconia balls and ethanol as media for 24 h to crush agglomerates and to minimize the particle size. The calcined fine powders were mixed with 5 wt% polyvinyl alcohol (PVA, as binder) and were pressed into pellets of 12 mm diameter and 2–3 mm thickness using steel die and hydraulic press with uniaxial pressure of 700–900 kg/cm^2. Binder was burned off at 500 °C for 3 h and the green bodies were sintered at 1225 °C for 4 h. The sintering process was conducted in a lead-rich environment and fired in closed alumina crucibles to minimize lead oxide volatilization. After sintering process, the samples were cooled to the room temperature along with furnace.

2.2 Structural characterization

X-ray diffractometer (XRD: Model PW-1710 Philips powder X-ray diffractometer) with CuK_α radiation with Ni filter at room temperature was used to characterize phase change in sintered specimens. The XRD were recorded at a scan rate of 1°/min and 2θ = 20–60°. As-sintered nano-ceramic surfaces were polished, thermally etched at 1025 °C for 1 h and gold coated using a sputtering technique to analyze microstructure. The microstructural studies were observed through scanning electron microscopy (SEM) of JEOL Model JSM 840A. Fractured surfaces of the nano-ceramics were also coated with gold for SEM studies. The grain sizes were measured by the linear interception method [22] with scanning electron micrographs. The particle size of the calcined powder was studied by using a transmission electron microscope JEOL JEM 1200. The apparent densities of sintered nano-ceramics were measured using the Archimedes method.

2.3 Electrical characterization

The lapped pellets were electroded with silver paste painted on both faces of pellets to form perfect electrodes and fired

at 600 °C for 1 h. The electroded specimens were characterized for room temperature dielectric constant (ε_{RT}), dielectric maximum (ε_{Tc}), Curie temperature (T_c) and dissipation factor (Tanδ) at 1 kHz using 4192A HP Impedance Analyzer. In this study, the temperature change was provided by an automatic temperature chamber (Delta 2300).

The electroded specimens were poled in a silicon oil bath at 100 °C by applying a dc field of 20 kV/cm. After 24 h ageing, the poled specimens were characterized for piezoelectric properties. The piezoelectric planar coupling coefficients (k_p) of the poled samples were characterized using a HP-4192A impedance analyzer through the resonance and anti-resonance technique. The piezoelectric charge coefficients (d_{33}) were characterized using a Berlincourt piezo-d-meter.

3 Results and discussion

3.1 XRD studies of Mn modified PLBSZZNT ceramics

X-ray diffraction patterns of undoped and Mn modified PLBSZZNT is depicted in Fig. 1a–c. XRD studies revealed that isovalent Ba^{2+} and Sr^{2+} doping at A-site and pentavalent donor Nb^{5+}, acceptors Zn and Mn at B-site in PLZT (MPB composition) lattice resulted in tetragonality, and increasing Mn concentration led to highly intensified tetragonal symmetry. The isovalent ions Ba^{2+} and Sr^{2+} partially substitute Pb^{2+} at A-site and pentavalent donor Nb^{5+} and acceptors Zn^{2+} and Mn^{4+} partially substitute Zr^{4+}/Ti^{4+} at B-site due to the approximately close and similar ionic radii of respective cations at A-site and B-site in PLZT lattice. It holds good that in pure PLZT or undoped PLZT composition at the MPB, there is coexistence of both rhombohedral and tetragonal phases (depends on Zr/Ti ratio), whereas, this may not hold good (coexistence of FE_{RH} and FE_{TET} phases) due to the effect of the (i) nature, (ii) amount (iii) type of dopant as well as (iv) Zr/Ti ratio. Hence, isovalent Ba^{2+} and Sr^{2+} at A-site and Nb^{5+}, Zn^{2+} and Mn^{4+} at B-site in the perovskite strengthen the moderate tetragonal phase to intensified tetragonality. The undoped composition exhibit broadened peak at h = 0 while peak splitting with strong tetragonality for h = 1.5 mol% Mn near $2\theta = 43.97°$ of {002}and 44.77° of {200} and $2\theta = 55.06°$ of {112} and 55.32° of {211} which indicates extraordinary tetragonal structure (FE_{TET}). In this study, the MPB has been taken as Zr:Ti = 53:47 where XRD patterns indicate a FE_{TET} at undoped composition and the sharp highly intensified tetragonal peak splitting with increasing Mn modification in PLBSZZNT lattice. The ionic radii of Sr^{2+} and La^{3+} are slightly smaller than that of Pb^{2+} and Ba^{2+}, while Nb^{5+}, Zn^{2+} and Mn^{4+} radii is approximately similar to the B-site (Zr^{4+}/Ti^{4+}) resulting in extraordinary intensified tetragonality. Please refer Table 2 for ionic radius [23].

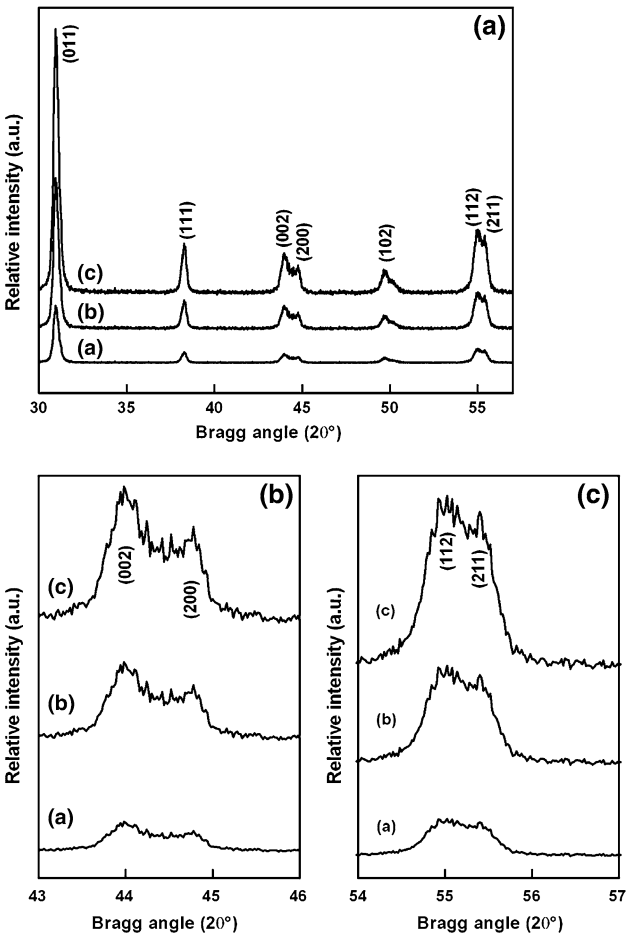

Fig. 1 (**a–c**) XRD patterns of undoped and Mn modified PLBSZZNT ceramics

Table 2 Ionic radii of different cations [23]

Cations	Ionic radii (Å)
Pb^{2+}	1.49
La^{3+}	1.36
Ba^{2+}	1.61
Sr^{2+}	1.44
Zr^{4+}	0.89
Ti^{4+}	0.74
Nb^{5+}	0.74
Zn^{2+}	0.90
Mn^{4+}	0.83

3.2 Microstructure and density studies of Mn modified PLBSZZNT ceramics

Figure 2a shows the average grain size and apparent density of undoped and Mn modified PLBSZZNT ceramics, respectively. Figure 2b shows SEM of 0.5 mol% Mn

modified PLBSZZNT nano-ceramic. Figure 2c shows Transmission Electron Micrograph of 0.5 mol% Mn modified PLBSZZNT nano-ceramic. The transmission electron microscopy (TEM) studies for calcined powders revealed that fine and semi-agglomerated nano ceramic powders with particle size ranging from 20 to 72 nm. The properties of PLZT are known to be effected by the following features viz., type, nature and amount of doping elements. Particularly, donor elements like Sr, Ba on Pb-site, or Nb on Zr,Ti-site have been reported for their enhanced electrical features [3]. The materials average grain size was determined directly from the SEM micrographs by using the classical linear interception method [21]. It is observed that a small amount of Mn concentration reduces the oxygen vacancies mobility resulting in homogeneous distribution in the PLZT perovskite structure. The doping on A (Pb) site with isovalent Ba^{2+} and Sr^{2+}, and B (Zr,Ti) site with pentavalent donor Nb^{5+} and acceptors Zn^{2+} and Mn^{4+} elements influences the microstructure development and electrical properties of the nano-ceramics. The isovalent dopants Sr^{2+}, Ba^{2+}, donor Nb^{5+} acceptor dopants Zn^{2+} and Mn^{4+} are expected to reduce the oxygen vacancies mobility in the PLZT lattice and therefore reduce the concentration of domain-stabilizing defect pairs. The term element substitution means that cations in a perovskite lattice, i.e. Pb^{2+}, Zr^{4+} and Ti^{4+} are replaced partially by other cations with the approximately same chemical valence and similar ionic radii as those of the replaced ions. The new substitution cation usually occupies the position of the replaced cation in the perovskite lattice and a substitutional solid solution is thus formed. Substitutions may cause an increase in the density of PLZT ceramics owing to the fluxing of isovalent substitutions Sr and Ba at the A-site, and, donor Nb and acceptors Zn^{2+} and Mn^{4+} at the B-site, during the period of sintering, which facilitates the process of atomic diffusion rapidly, hence the densification occurs in the ceramics. In the case of multiple cation modified piezoelectric ceramic systems, dielectric and piezoelectric properties of ceramics are also improved by substitution of Pb at A-site and Zr/Ti at B-site by several acceptor and donor cations. It has been reported that the density rapidly increased due to the formation of lattice vacancies by the diffusion of Mn [24]. The factors influencing density are: (i) the complete chemical reaction which is promoted with the existence of multiple cations in the perovskite [25], (ii) (Ba-Sr-Nb-Zn-Mn) in PLZT perovskite that led to high ionic polarization within the lattice and (iii) the excess 5 wt% of PbO addition led to the prevention of Pb loss during high temperature sintering and promoting density as shown in SEM picture. The density increased with the presence of multiple ions and as Mn content increased, the density enhanced from h = 0 mol % (7.49 gm/cm^3) to h = 1.5 mol % (7.73 gm/cm^3).

3.3 Dielectric behavior of Mn modified PLBSZZNT ceramics

Figure 3a–d shows room temperature dielectric constant (ε_{RT}), Curie temperature (T_c), dielectric loss ($Tan\delta_{RT}$ and $Tan\delta_{Tc}$) and dielectric maximum (ε_{Tc}) of undoped and Mn modified PLBSZZNT ceramics at 1 kHz, respectively. As shown in Fig. 3a, the room-temperature dielectric constant increased with increasing Mn content and exhibited a maximum value of 2946 at h = 1.5 mol% Mn, which can be attributed to the effect of multiple ions, resulting in a relatively high dielectric constant. Also an increase of the dielectric constant is associated with reduction of the Curie temperature, resulting from possible substitution of Sr and Ba into Pb-site and Nb, Zn and Mn into the Zr/Ti-site in the PLZT nano-ceramics. A higher dielectric maximum (18492 at 1 kHz) has been observed in 1 mol% Mn while the Curie temperature shifted towards lower temperature with a decreasing dielectric loss at room temperature in the series. The degree of the T_c shift was 248 °C from undoped to 218 °C of 1.5 mol% Mn as can be observed from Fig. 3b. The dielectric loss ($Tan\delta_{RT}$) gradually decreased from undoped to 1 mol% Mn while ($Tan\delta_{Tc}$) constantly increased in the series. The reduced oxygen vacancy concentration could also lead to improved reliability, as oxygen vacancy migration is considered the major cause of degradation in perovskites and Mn reduces the oxygen vacancy migration to charge balance in the perovskite [26]. The pentavalent donor Nb^{5+} additive and isovalent Ba^{2+} and Sr^{2+} enhance domain reorientation resulting in high dielectric permittivity. The isovalent (Ba and Sr) and acceptors (Zn and Mn) substitutions attribute to the highly intensified tetragonality that explains the increase of dielectric permittivity [9, 12, 18, 27].

3.4 Piezoelectric properties of Mn modified PLBSZZNT ceramics

Figure 4 shows the piezoelectric planar coupling coefficients (k_p) and the piezoelectric charge coefficients (d_{33}) of the poled undoped and Mn modified PLBSZZNT ceramics characterized through a HP-4192A impedance analyzer by resonance and anti-resonance technique and Berlincourt piezo-d meter, respectively. The influence of Ba and Sr at A-site, and Nb^{5+}, Zn^{2+} and Mn^{4+} at B-site on the piezoelectric properties of lead lanthanum zirconate titanate (PLZT, close to the morphotropic phase boundary) nano-ceramics is investigated. In general, piezoelectric properties of ceramics increase approximately linearly with increasing grain size. The dependence of piezoelectric properties on average grain size in the modified PZT ceramic has been investigated [28]. It has been observed

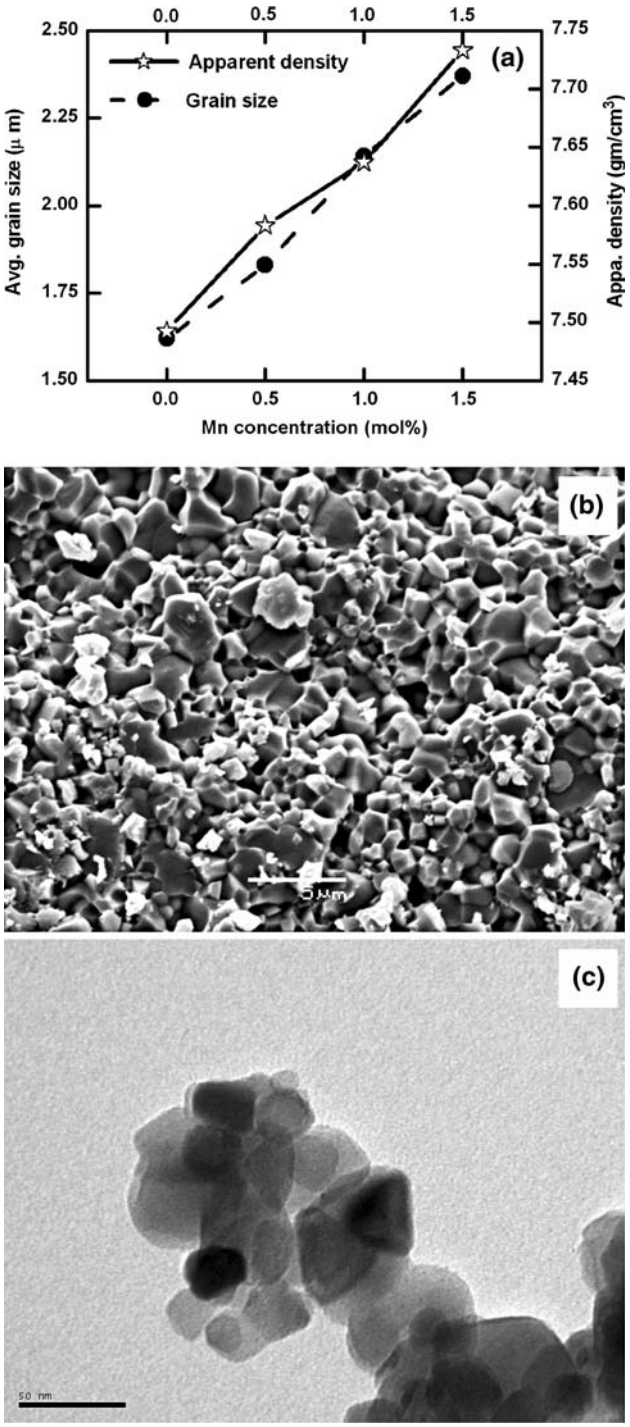

Fig. 2 (**a**) Average grain size and apparent density profile of undoped and Mn modified PLBSZZNT ceramics. (**b**) Scanning electron micrograph of 0.5 mol% Mn modified PLBSZZNT nano-ceramic. (**c**) Transmission electron micrograph of 0.5 mol% Mn modified PLBSZZNT nano-ceramic

that Zn modification causes the creation of oxygen vacancies and isovalent substitutions causes lead vacancies, while donor Nb modification influences charge/oxygen vacancy formation and Mn modification reduces the oxygen vacancies mobility to balance the charge in PLZT perovskite. The properties of piezoelectric PLZT ceramics are influenced by the domain reorientation caused by the presence of multiple ions in the perovskite. Moreover, isovalent substitutions are very sensitive with respect to piezoelectric properties. However, it has been observed that the combination of both multiple donor and acceptor modification in the PLBSZZNT perovskite with Mn content variation that reduced the oxygen vacancies mobility while balancing the charge in the lattice. As a result, high piezoelectric coefficients were achieved [29, 30]. Furthermore, the multiple ions modification (Ba^{2+}, Sr^{2+}, Nb^{5+}, Zn^{2+} and Mn^{4+}) in the PLZT lattice facilitates grain growth enhancement in the nano-ceramics influencing domain orientation and thus, resulted in enhanced piezoelectric properties. Thus, the piezoelectric planar coupling coefficient k_p = 0.452 to 0.567 and the piezoelectric charge coefficient d_{33} = 376 to 486 pC/N increased from undoped to 1.5 mol% Mn, respectively in the PLBSZZNT ceramics.

4 Conclusion

Introduction of isovalent Ba^{2+} and Sr^{2+} to the Pb-site, and pentavalent donor Nb^{5+}, acceptors Zn^{2+} and Mn^{4+} at the Zr/Ti-site was carried out to balance the charge as well as the oxygen vacancies in the PLZT perovskite to obtain a relatively enhanced dielectric and piezoelectric properties. The transmission electron microscopy (TEM) studies for calcined powders revealed that fine and semi-agglomerated nano ceramic powders with particle size ranging from 20 to 72 nm. Microstructural characteristics resulting from as-prepared nano ceramic compositions were found to depend strongly on the content of multiple ions which resulted in increased grain growth, while promoting apparent density. The multiple ions both at A-site and B-site enhanced the dielectric constant while decreasing the Curie temperature (T_c). The isovalent ions Ba^{2+} and Sr^{2+} partially substitute Pb^{2+} at A-site, and pentavalent donor Nb^{5+} and acceptors Zn^{2+} and Mn^{4+} partially substitute Zr^{4+}/Ti^{4+} at B-site, due to the approximately close and similar ionic radii of respective cations that influenced highly intensified tetragonality. The decrease in Curie temperature and increase in dielectric constant can be attributed to the emerging lead vacancies creation by donor cations, and acceptor Mn to reduce the oxygen vacancies mobility to balance charge in the modified PLZT perovskite. It has been observed that Zn modification causes the creation of oxygen vacancies and isovalent substitutions causes lead vacancies, while Nb modification influences vacancy formation and Mn modification reduces the oxygen vacancies mobility to balance the charge in the modified PLZT perovskite. Thus, optimum piezoelectric properties

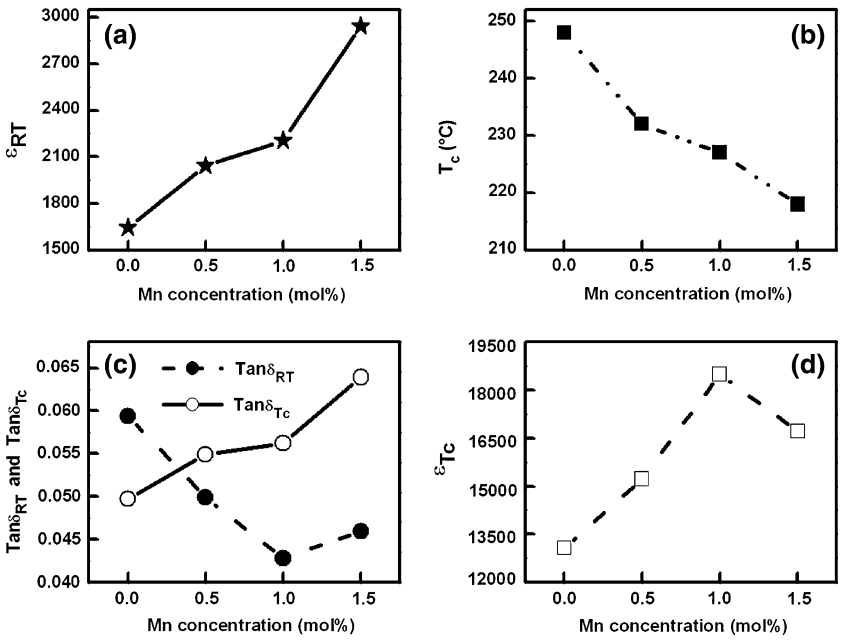

Fig. 3 (**a**) Room temperature dielectric constant (ε_{RT}), (**b**) Curie temperature (T_c), (**c**) dielectric loss ($Tan\delta_{RT}$ and $Tan\delta_{Tc}$) and (**d**) dielectric maximum (ε_{Tc}) of undoped and Mn modified PLBSZZNT ceramics at 1 kHz, respectively

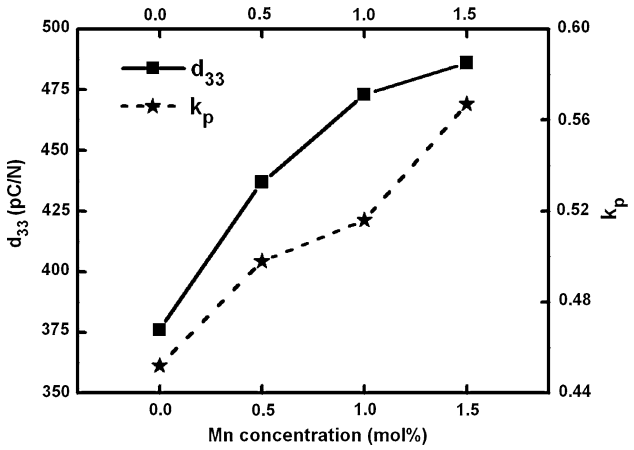

Fig. 4 Piezoelectric properties (k_p and d_{33}) of undoped and Mn modified PLBSZZNT ceramics

achieved in 1.5 mol% Mn modified PLBSZZNT nano-ceramics may be suitable for possible sensor and actuator applications.

Acknowledgments The authors would like to thank University of Concepcion for their financial assistance extended, Mr. Ranganathan and Ms. C. N. Devi for their technical assistance extended during this work.

References

1. G.H. Haertling, in *Electro-optic Ceramics and Devices in Electronic Ceramics*, ed. by L.M. Levinson (Marcell Dekker, Inc., New York, 1988), p. 201
2. Y. Xu, *Ferroelectric Materials and Their Applications* (The Netherlands, North Holland, 1991), p. 110
3. B. Jaffe, W.R. Cook, H. Jaffe, *Piezoelectric Ceramics* (Academic Press, London, 1971), p. 135
4. A. Dalakoti, A. Bandyopadhyay, S. Bose, J. Am. Ceram. Soc. **89**(3), 1140 (2006)
5. K. Ramam, M. Lopez, J. Phys. D: Appl. Phys. **39**, 4466 (2006)
6. J. Ryu, J.J. Choi, H.E. Kim, J. Am. Ceram. Soc. **84**(4), 902 (2001)
7. S. Priya, K. Uchino, J. Ryu, C.W. Ahn, S. Nahm, Appl. Phys. Lett. **83**(24), 5020 (2003)
8. M.E. Mendoza, A.P. Barranco, O.G. Zaldivar, R.L. Noda, F.C. Pinar, Ferroelectrics. **334**, 35 (2006)
9. Z. Zhu, N. Zheng, G. Li, Q. Yin, J. Am. Ceram. Soc. **89**(2), 717 (2006)
10. K. Ramam, S.H. Luis, Eur. Phys. J. Appl. Phys. **35**, 49 (2006)
11. C.B. Yoon, Y.H. Koh, G.T. Park, H.E. Kim, J. Am. Ceram. Soc. **88**(6), 1625 (2005)
12. A. Banerjee, A. Bandyopadhyay, S. Bose, Ceram. Trans. (CT), Ceram. Nanomater. Nanotech. **III**, 159 (2004)
13. Y. Uesu, M. Matsuda, Y. Yamada, K. Fujishiro, D.E. Cox, B. Noheda, G. Shirane, J. Phys. Soc. Jpn. **71**, 960 (2002)
14. J. Yoo, Y. Lee, K. Yoon, S. Hwang, S. Suh, J. Kim, C. Yoo, Jpn. J. Appl. Phys. **1**(40), 3256 (2001)
15. P.M. Gehring, S.E. Park, G. Shirane, Phys. Rev. Lett. **84**, 5216 (2000)
16. M. Villegas, A.C. Caballero, C. Moure, P. Duran, J.F. Fernandez, R.E. Newnham, J. Am. Ceram. Soc. **83**(1), 141 (2000)
17. S.B. Majumder, B. Perez, B. Roy, A. Martinez, R.S. Katiyar, Mat. Res. Soc. Symp. Proc. **655**, CC12.14.1–CC12.14.6 (2001)
18. S.K.S. Parashar, R.N.P. Choudhary, B.N. Murty, Ferroelectrics. **325**, 65 (2005)
19. T. Akahsi, N. Tsubouchi, M. Takahashi, T. Ohno, U.S. Patent 3,461,071, 1969
20. N. Uchida, T. Ikeda, Jpn. J. Appl. Phys. **6**, 1292 (1967)
21. Q. Zhang, R.W. Whatmore, J. Phys. D. Appl. Phys. **34**(15), 2296 (2001)
22. M.I. Mendelson, J. Am. Ceram. Soc. **52**, 443 (1969)
23. R.D. Shannon, Acta Cryst. **A32**, 751 (1976)
24. J.J. Choi, S.W. Kim, H.E. Kim, J. Am. Ceram. Soc. **85**(3), 733 (2002)
25. L.B. Kong, J. Ma, W. Zhu, O.K. Tan, Scripta Mater. **44**, 345 (2001)

26. Q. Zhang, R.W. Whatmore, J. Eur. Ceram. Soc. **24**(2), 277 (2004)
27. A. Banerjee, A. Bandyopadhyay, S. Bose, J. Am. Ceram. Soc. **89**(5), 1594 (2006)
28. K. Okazaki, K. Nagata, J. Electron. Commun. Soc. Jpn. **C53**, 815 (1970)
29. E. Boucher, D. Guyomar, L. Lebrun, B. Guiffard, G. Grange, J. Appl. Phys. **92**(9), 5437 (2002)
30. B. Guiffard, E. Boucher, L. Lebrun, D. Guyomar, E. Pleska, Ferroelectrics. **313**, 135 (2004)